Calculation of Photon Dispersion Relations

J. B. Pendry and A. MacKinnon
The Blackett Laboratory, Imperial College, London SW7 2BZ, United Kingdom
(Received 2 April 1992)

The current generation of photon scattering experiments requires a fast, accurate, general technique for calculation of transmission coefficients and of photonic band structure. A new methodology, which has significant advantages of speed and convenience, enables the band structure and, for the first time, transmission coefficients of complex dielectric materials to be calculated. Excellent agreement with experiment is found.

PACS numbers: 41.20.Jb, 71.25.Cx, 84.90.+a

The formation of allowed and forbidden bands of frequency is a phenomenon common to all wavelike disturbances in periodic media. Only the case of electrons in crystalline solids has been extensively studied, but recently Yablonovitch and co-workers [1,2] have published a striking analogy between the electron band gap in an insulator and a gap in the photon spectrum of a periodic dielectric. These experiments are strongly motivated by theoretical considerations, so there is an urgent need to set photonic band theory on the same firm basis as electron band structure. A few pioneering papers have already appeared [2–5] and conclude that photons constitute a nontrivial extension of the electron case: The vector nature of the field, particularly the need to exclude the unphysical longitudinal modes, needs to be addressed carefully. The theories developed in [2–5] have been highly successful in accounting for Yablonovitch's data, but there remain important gaps in our computational capability and it is these which we address in this Letter:

(i) A wave of fixed frequency ω incident on a periodic dielectric in principle excites all bands at that frequency. Current methodologies calculate ω given a real $\mathbf{k}$, and the search for complex $\mathbf{k}$ is nontrivial. What is required is the photon equivalent of the on-shell scattering methodologies employed in low-energy electron diffraction theory to calculate all the bands $\mathbf{k}(\omega)$, real and complex [6].

(ii) For highly complex structures such as disordered systems, or periodic structures containing a single defect or "dopant" (see [2]), Fourier methods are extremely time consuming. In contrast, on-shell methodologies expand the wave field over a *surface*, not a *volume*, and hence give a more compact description, and a much more efficient calculation. All calculations of electron reflection and transmission coefficients are made by on-shell methods of one sort or another.

(iii) The current theories all work in Fourier space, and require a well-defined Fourier expansion of the dielectric constant $\varepsilon(\mathbf{r})$. For metallic systems at microwave frequencies, $\varepsilon(\mathbf{r})$ takes on very large imaginary values and Fourier methods become impractical.

Further impetus is added by the desire to exploit the electron-photon analogy to study disordered systems [7]. Several experiments have been made on the interaction of photons with strongly disordered dielectric media. In the optical backscattering experiments [8,9], photons moving in a disordered medium show the same backscattering peak as predicted for electrons by the maximally crossed diagrams, while Genack and Garcia [10] have used microwaves as a powerful probe of localization effects in disordered media.

In this Letter we seek to establish the computational framework within which photonic phenomena can be studied with the same facility now available for electrons. Our method is in essence a finite-element method in which space is divided into a set of small cells with coupling between neighboring cells. For most materials ε can be treated as diagonal in real space and hence complex structures can readily be incorporated into this methodology, even those including regions where $\varepsilon=\infty$.

The choice of lattice and of coupling elements is crucial to the stability of the method. Excellent stability can be achieved provided certain requirements are met. In the electron case this amounts to requiring that, as the cell size tends to zero, all low-frequency modes converge to the continuum limit. Of course the modes at higher frequencies may still be in serious error, but they pose no problems provided that the system is never subjected to these high frequencies. Some choices of cell do not have this property and are plagued by low-frequency "ghosts." In the electromagnetic case we are presented with a particular problem in this respect: The longitudinal solutions of Maxwell's equations can be regarded as a set of zero-frequency modes with no dispersion; at finite frequencies they are present in principle but only as waves decaying infinitely rapidly. Finite-element models in which the longitudinal modes are only *approximately* zero will inevitably confuse longitudinal with low-frequency transverse modes—just the ones we should be calculating most accurately. Therefore a requirement of our model is that it must contain a set of modes which at all cell sizes have zero frequency and are nondispersing, and which in the limit of small cell size converge to the longitudinal modes.

We start from Maxwell's equations,

$$\nabla\times\mathbf{E}=-\partial\mathbf{B}/\partial t\,, \tag{1}$$

$$\nabla\times\mathbf{H}=\partial\mathbf{D}/\partial t\,, \tag{2}$$

and assume that

$$\mathbf{B}=\mu_0\mathbf{H}; \tag{3}$$

hence,

$$\nabla\times\nabla\times\mathbf{E}=-\mu_0\partial^2\mathbf{D}/\partial t^2=\varepsilon(\mathbf{r})c^{-2}\partial^2\mathbf{E}/\partial t^2$$
$$=-\nabla^2\mathbf{E}+\nabla(\nabla\cdot\mathbf{E}). \tag{4}$$

Transforming to $(\mathbf{k},\omega)$ space,

$$(\mathbf{k}\cdot\mathbf{k})\mathbf{E}(\mathbf{k})-\mathbf{k}[\mathbf{k}\cdot\mathbf{E}(\mathbf{k})]=\omega^2c^{-2}\sum_{\mathbf{k}'}\varepsilon(\mathbf{k},\mathbf{k}')\mathbf{E}(\mathbf{k}'). \tag{5}$$

Note the outer product in the second term $\{\mathbf{k}[\mathbf{k}\cdot\mathbf{E}(\mathbf{k})]=(\mathbf{k}\otimes\mathbf{k})\cdot\mathbf{E}(\mathbf{k})\}$ on the left-hand side: Its function is to ensure that the longitudinal modes have zero frequency. Any mode that is polarized perpendicular to $\mathbf{k}$ obeys the normal Laplacian equation. The strategy we employ is to discretize this equation, approximating $\mathbf{k}\cdot\mathbf{k}$ and $\mathbf{k}\otimes\mathbf{k}$ by sines and cosines. By retaining the form of an outer product we ensure that one of the three modes is always of zero frequency and therefore plays no part in transport. On transforming back into real space, expressions like $\exp(ik_xa)$ give rise to terms coupling to some neighbor. The lattice structure is defined by the choice of approximation, as is the occurrence of first, second, etc., nearest neighbors. Approximate (5) by

$$a^{-2}\sum_j([|\exp(ik_xa)-1|^2+|\exp(ik_ya)-1|^2+|\exp(ik_za)-1|^2]\delta_{ij}-\{[\exp(ik_ia)-1][\exp(-ik_ja)-1]\})E_j$$
$$=\omega^2c^{-2}\sum_{\mathbf{k}'}\varepsilon(\mathbf{k},\mathbf{k}')E_i(\mathbf{k}'). \tag{6}$$

On transforming back into real space we get 3×3 blocks of elements relating to sites on a simple cubic lattice, extending to next-nearest-neighbor interactions. However, it is advantageous to stay with a set of coupled first-order equations for the $\mathbf{E}$ and $\mathbf{H}$ fields when it comes to a numerical implementation of the formulas. Transforming (1) and (2) into $(\omega,\mathbf{k})$ space, we have

$$\mathbf{k}\times\mathbf{E}=+\omega\mathbf{B}, \tag{7}$$

$$\mathbf{k}\times\mathbf{H}=-\omega\mathbf{D}. \tag{8}$$

In (7) we approximate,

$$k_x\approx(ia)^{-1}[\exp(ik_xa)-1],\ \text{etc.}, \tag{9}$$

and in (8),

$$k_x\approx(-ia)^{-1}[\exp(-ik_xa)-1],\ \text{etc.} \tag{10}$$

Transforming back into real space gives a set of equations from which the z components of the vectors can be eliminated, and the substitution

$$\mathbf{H}'=+(i/a\omega\varepsilon_0)\mathbf{H} \tag{11}$$

made, to give

$$E_x(\mathbf{r}+\mathbf{c})=+\frac{a^2\omega^2}{c^2}\mu(\mathbf{r})H_y'(\mathbf{r})+E_x(\mathbf{r})$$
$$+\varepsilon^{-1}(\mathbf{r})[H_y'(\mathbf{r}-\mathbf{a})-H_y'(\mathbf{r})-H_x'(\mathbf{r}-\mathbf{b})+H_x'(\mathbf{r})]$$
$$-\varepsilon^{-1}(\mathbf{r}+\mathbf{a})[H_y'(\mathbf{r})-H_y'(\mathbf{r}+\mathbf{a})-H_x'(\mathbf{r}+\mathbf{a}-\mathbf{b})+H_x'(\mathbf{r}+\mathbf{a})], \tag{12}$$

$$E_y(\mathbf{r}+\mathbf{c})=-\frac{a^2\omega^2}{c^2}\mu(\mathbf{r})H_x'(\mathbf{r})+E_y(\mathbf{r})$$
$$+\varepsilon^{-1}(\mathbf{r})[H_y'(\mathbf{r}-\mathbf{a})-H_y'(\mathbf{r})-H_x'(\mathbf{r}-\mathbf{b})+H_x'(\mathbf{r})]$$
$$-\varepsilon^{-1}(\mathbf{r}+\mathbf{b})[H_y'(\mathbf{r}-\mathbf{a}+\mathbf{b})-H_y'(\mathbf{r}+\mathbf{b})-H_x'(\mathbf{r})+H_x'(\mathbf{r}+\mathbf{b})], \tag{13}$$

$$H_x'(\mathbf{r}+\mathbf{c})=\varepsilon(\mathbf{r}+\mathbf{c})E_y(\mathbf{r}+\mathbf{c})+H_x'(\mathbf{r})$$
$$-\frac{c^2}{a^2\omega^2}\mu^{-1}(\mathbf{r}-\mathbf{a}+\mathbf{c})[E_y(\mathbf{r}+\mathbf{c})-E_y(\mathbf{r}-\mathbf{a}+\mathbf{c})-E_x(\mathbf{r}-\mathbf{a}+\mathbf{b}+\mathbf{c})+E_x(\mathbf{r}-\mathbf{a}+\mathbf{c})]$$
$$+\frac{c^2}{a^2\omega^2}\mu^{-1}(\mathbf{r}+\mathbf{c})[E_y(\mathbf{r}+\mathbf{a}+\mathbf{c})-E_y(\mathbf{r}+\mathbf{c})-E_x(\mathbf{r}+\mathbf{b}+\mathbf{c})+E_x(\mathbf{r}+\mathbf{c})], \tag{14}$$

$$H_y'(\mathbf{r}+\mathbf{c})=-\varepsilon(\mathbf{r}+\mathbf{c})E_x(\mathbf{r}+\mathbf{c})+H_y'(\mathbf{r})$$
$$-\frac{c^2}{a^2\omega^2}\mu^{-1}(\mathbf{r}-\mathbf{b}+\mathbf{c})[E_y(\mathbf{r}+\mathbf{a}-\mathbf{b}+\mathbf{c})-E_y(\mathbf{r}-\mathbf{b}+\mathbf{c})-E_x(\mathbf{r}+\mathbf{c})+E_x(\mathbf{r}-\mathbf{b}+\mathbf{c})]$$
$$+\frac{c^2}{a^2\omega^2}\mu^{-1}(\mathbf{r}+\mathbf{c})[E_y(\mathbf{r}+\mathbf{a}+\mathbf{c})-E_y(\mathbf{r}+\mathbf{c})-E_x(\mathbf{r}+\mathbf{b}+\mathbf{c})+E_x(\mathbf{r}+\mathbf{c})]. \tag{15}$$

The simple cubic mesh on which we define the fields is defined by vectors **a**,**b**,**c**, of length a which point in the x,y,z directions, respectively. The first two equations (12) and (13) express the **E** field on the next plane of cells in terms of the **E** and **H** fields on the previous plane. The second pair of equations (14) and (15) express the **H** fields on the next plane of cells in terms of the **E** on the same plane, and the **H** fields on the previous plane. Thus, given the x,y components of the **E** and **H** fields on one side of a dielectric structure, we can integrate through the structure to find the x,y components of the **E** and **H** fields on the other side. Incidentally, if we wish, we can also use subsidiary equations to calculate the z components too. The matrix relating fields on one side of a structure to those on the other is by definition the *transfer matrix*. Where the structure is the unit cell of a periodic array, the eigenvalues of the transfer matrix give the band structure of the system [6,11–13]. Using this transfer matrix gives our calculations some distinct advantages: For a dielectric structure containing $L\times L\times L$ cells the dimensions of the transfer matrix are $4L^2$, giving the compact representation we expect of an on-shell method. Current methods would need to diagonalize a matrix of dimensions $2L^3$; thus our method has an advantage in speed of $(2L^3)^3/(4L^2)^3=L^3/8$, or a factor more than 10^2 when $L=10$.

There is an elegant reformulation of these equations that gives considerable geometric insight into the problem. Consider two interpenetrating simple cubic lattices such that the two lattices together constitute a bcc lattice. The first lattice we associate with the electric field **E**, and the second with the magnetic field **B**. The x,y,z components of the **E** field are each associated with the bonds leaving the lattice sites in the $+x,+y,+z$ directions, with a similar decomposition for the **B** field. Equations (1) and (2) can be reexpressed in integral form via the Stokes theorem:

$$\int \mathbf{E}\cdot d\mathbf{l} = -\int (\partial\mathbf{B}/\partial t)\cdot d\mathbf{S}\,, \tag{16}$$

$$\int \mathbf{H}\cdot d\mathbf{l} = +\int (\partial\mathbf{D}/\partial t)\cdot d\mathbf{S}\,. \tag{17}$$

Observe that each bond carrying a component of **B** threads through a square of bonds carrying the **E** field, and we apply the first equation to this circuit. In an exactly complementary fashion we can relate **D** to **H** using the second of these equations. This procedure can easily be shown to give the same dispersion relations as our first algebraic derivation. With appropriate choice of parameters the mesh can easily be topologically distorted to vary the density of sampling points.

Advancing the **E** and **H** fields through a single slice involves multiplication by a sparse matrix. Thus we can iterate Eqs. (12)–(15) very efficiently to calculate the transmission coefficient directly [14], or to give the band structure $\mathbf{k}(\omega)$ by diagonalizing the transfer matrix.

We have made calculations for a periodic array of dielectric cylinders, diameter 0.74 mm, $\varepsilon=8.9$, and arranged in a square lattice with spacing $a=1.87$ mm. These parameters were chosen because there are experimental measurements of transmission coefficients and band structure available made using the coherent microwave transient spectroscopy (COMITS) technique [15]. For our calculations the unit cell of the system was divided into a $10\times10\times1$ mesh: For each cell an average was taken over the dielectric constant within that cell. The transfer matrix was found by multiplying the matrices for each of the ten slices. Its eigenvalues give $k_z(\omega,k_x,k_y)$. For the transmission coefficient a similar division of the cell was made, but multiplying transfer matrices for the seven layers of unit cells would have led to numerical instability, so, instead, multiplication was halted after integrating through one unit cell at which point the transmission and reflection coefficients were calculated for a slab one cell thick. Slabs were then stacked together using the multiple scattering formula familiar in the theory of low-energy electron diffraction [6]. Convergence was tested by repeating the calculation for a $20\times20\times1$ mesh: Changes of the order of 1% at 80 GHz were found in the band structure.

Our method proved numerically stable: Current conservation was obeyed to at least five decimal places (as many as were printed out) and was fast enough that the bands could easily be calculated on a personal computer. Moving the codes to our RISC workstations provides us with an extremely powerful desktop vehicle for investigation of photonic band structure.

Figure 1 shows the band structure. The frequency of bands scales linearly with system size, so corresponding structures fabricated on a micron scale would give band gaps in the optical region of the spectrum. Data from [15] are shown as black dots and agree with calculations to within experimental resolution of 5 GHz. Note the radical distortion of the dispersion relations, particularly near the band edges where the group velocity vanishes, all of which is in agreement with experiment. Bands more narrow than 5 GHz are not resolved experimentally.

Figure 1 also shows for the first time a calculated transmission coefficient: For the dielectric array described above, truncated at a thickness of seven rows of cylinders, propagation is in the (10) direction. Polarization is conserved by symmetry and scattering is strongest when **E** is parallel to the cylinders as evidenced by the large band gap observed in Fig. 1(b) around 60 GHz. Note the much reduced transmission coefficient around this frequency. In the band gap waves are exponentially attenuated in the periodic structure. A smaller feature at around 100 GHz is also seen. The much smaller band gaps in Fig. 1(a) around 70 and 110 GHz produce similar minima. Notice the oscillatory structure on the theoretical curves: These are Fabry-Pérot resonances caused by waves multiply scattering between entry and exit surfaces of the periodic dielectric. They are not resolved in the experiment: The pulse of microwaves was

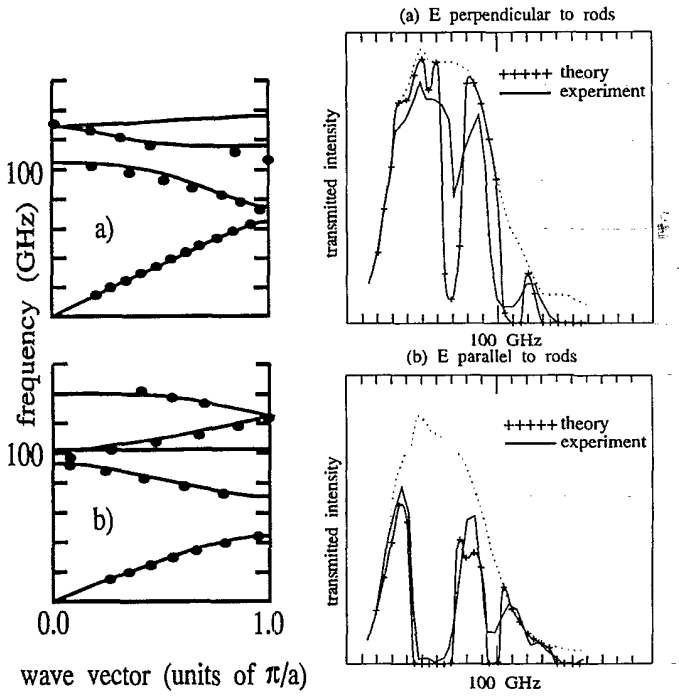

FIG. 1. Left: dispersion relation for propagation of electromagnetic waves along the (10) direction of a 2D array of dielectric cylinders. (a) E perpendicular to the cylinders; (b) E parallel to the cylinders. The experimental results are shown as black dots and have a resolution of 5 GHz. Note that very narrow bands are not resolved experimentally. Right: transmitted power for an array of seven rows of dielectric cylinders. The dotted curve shows the instrument response in the absence of the cylinders. (a) E perpendicular to the cylinders; (b) E parallel to the cylinders.

deliberately gated to exclude multiply scattered signals. Nevertheless, the spacing of this oscillatory structure in frequency gives an alternative way of estimating the dispersion of the bands from an experiment measuring intensities alone.

Agreement with experiment is most satisfying and gives us confidence that our method is capable of accurately reproducing experiments.

In conclusion, we have presented a new formalism for calculating the scattering of photons by complex dielectric structures which opens the field for simulations of all manner of systems, from photonic band structure of materials containing metallic elements, to calculation of transmission coefficients of arbitrary structures, to simulation of the properties of disordered dielectrics. The method successfully addresses the problems of eliminating the longitudinal modes, of numerical stability, and of speed of computation, in a formulation ideally suited to calculation of transmission coefficients. We have presented theoretical transmission coefficients, the first to be calculated, and successfully compared them to experiment.

We thank G. Arjavalingam for a very helpful discussion of his results.

[1] E. Yablonovitch, T. J. Gmitter, and K. M. Leung, Phys. Rev. Lett. **67**, 2295 (1991).
[2] E. Yablonovitch, T. J. Gmitter, R. D. Meade, A. M. Rappe, K. D. Brommer, and J. D. Joannopoulos, Phys. Rev. Lett. **67**, 3380 (1991).
[3] K. M. Leung and Y. F. Liu, Phys. Rev. Lett. **65**, 2646 (1990).
[4] Ze Zhang and Sashi Satpathy, Phys. Rev. Lett. **65**, 2650 (1990).
[5] K. M. Ho, C. T. Chan, and C. M. Soukoulis, Phys. Rev. Lett. **65**, 3152 (1990).
[6] J. B. Pendry, *Low Energy Electron Diffraction* (Academic, London, 1974).
[7] S. John, Phys. Rev. Lett. **58**, 2486 (1987).
[8] M. P. van Albada and A. Lagendijk, Phys. Rev. Lett. **55**, 2692 (1985).
[9] P. E. Wolf and G. Maret, Phys. Rev. Lett. **55**, 2696 (1985).
[10] A. Z. Genack and N. Garcia, Phys. Rev. Lett. **66**, 2064 (1991).
[11] J. B. Pendry, A. Prêtre, P. J. Rous, and L. Martín-Moreno, Surf. Sci. **244**, 160 (1991).
[12] A. MacKinnon, Z. Phys. B **59**, 385 (1985).
[13] A. MacKinnon and B. Kramer, Z. Phys. B **53**, 521 (1983).
[14] J. B. Pendry, A. MacKinnon, and P. J. Roberts, Proc. R. Soc. London A **437**, 67 (1992).
[15] W. M. Robertson, G. Arjavalingam, R. D. Meade, K. D. Brommer, A. M. Rappe, and J. D. Joannopoulos, Phys. Rev. Lett. **68**, 2023 (1992).